

The Electrospinning of Different Hemostatic Agents and Their Effectiveness

Başak ÜNVER KOLUMAN¹, Mahmed Sari NJJAR^{2*}, Ahmet KOLUMAN³

¹ Pamukkale University, Faculty of Medicine, Department of Hematology, Denizli, 20160, Türkiye.
e-posta: basakunver@yahoo.com, ORCID ID: 0000-0003-1106-5021

² Pamukkale University, Faculty of Technology, Department of Biomedical Engineering, Denizli, 20160, Türkiye.
e-posta: sari.njjar@hotmail.com, ORCID ID: 0000-0003-2494-1086

³ Pamukkale University, Faculty of Technology, Department of Biomedical Engineering, Denizli, 20160, Türkiye.
e-posta: ahmetkoluman@hotmail.com, ORCID ID: 0000-0001-5308-8884

www.dergipark.org.tr/rjbb

Received: 16.09.2023

Accepted: 13.11.2023

Keywords: *Astringents, Hemorrhage, Bleeding Time, Ankaferd Blood Stopper, Adrenaline, Tranexamic Acid*

Abstract

The purpose of this study is to present an effective solution for severe bleeding and tissue damage occurring during situations such as conflicts, disasters, and crises. The aim is to produce nanofibers that can serve as a hemostatic wound dressing, capable of both accelerating wound healing and controlling bleeding. Nanofibers are produced through the electrospinning method by combining hemostatic agents such as adrenaline (ADR), Transamin® (TXA), and Ankaferd Blood Stopper® (ABS) with polyvinyl alcohol (PVA) polymer. The morphology, chemical bonding structure, and hemostatic activity of these nanofibers are extensively analyzed. The feasibility of these nanofibers for medical applications, particularly as wound dressings, was investigated. Results: Field emission scanning electron microscopy (FESEM) images reveal that increased concentrations of adrenaline, TXA, and ABS result in the formation of beaded fibers. While ABS/PVA and TXA/PVA nanofibers have similar average diameters, ABS/PVA exhibits a more beaded morphology. According to hemostatic activity tests, clotting times were similar for adrenaline/PVA and TXA/PVA nanofibers, whereas ABS/PVA nanofibers exhibited a shorter clotting time. Among the findings, adrenaline/PVA nanofibers had the longest clotting time at 4.088 seconds. On the other hand, ABS/PVA nanofibers had the shortest clotting time at 3.819 seconds. An effective hemostatic agent should be able to stop bleeding within 2 minutes after application to the wound site in in vitro settings, without requiring mixing or preparation, and should be easily applicable to wounded areas. The developed hemostatic nanofibers demonstrated the ability to form clots within seconds. The resulting nanofibers from this study will not only contribute to public health but also significantly enhance survival processes.

Farklı Hemostatik Ajanların Elektroeğirme Yöntemiyle Üretimi ve Etkinliği

www.dergipark.org.tr/rjbb

Alınış Tarihi: 16.09.2023

Kabul Tarihi: 13.11.2023

Keywords: *Kanamayı Durdurucular, Kanama Zamanı, Ankaferd Kan Durdurucu, Adrenalin, Traneksamik Asit*

Özet

Bu çalışmanın amacı, çatışmalar, felaketler ve krizler gibi durumlar sırasında meydana gelen ciddi kanama ve doku hasarına yönelik etkili çözümler sunmak amacıyla hem yara iyileşmesini hızlandırabilen hem de kanamayı kontrol edebilen bir hemostatik yara örtüsü olarak kullanılabilir nanolifler üretmektir. Nanolifler, elektroeğirme yöntemiyle adrenalin (ADR), Transamin® (TXA) ve Ankaferd Blood Stopper® (ABS) gibi hemostatik maddeler ile polivinil alkol (PVA) polimerinin birleşimiyle elde edilmektedir. Çalışmada nanoliflerin morfolojisi, kimyasal bağ yapısı ve hemostatik aktivitesi ayrıntılı şekilde analiz edilmektedir. Bu nanoliflerin tıbbi uygulamalarda, özellikle yara örtüsü olarak kullanılabilirliği araştırılmıştır. Alan emisyonlu taramalı elektron mikroskobu (FESEM) görüntülerine göre, adrenalin, TXA ve ABS konsantrasyonunun artmasıyla boncuklu lifler oluşmaya başlamıştır. ABS/PVA ve TXA/PVA nanoliflerinin ortalama çapları aynı olmasına rağmen, ABS/PVA daha fazla boncuklu morfolojiye sahiptir. Hemostatik aktivite testlerine göre, adrenalin/PVA ve TXA/PVA nanoliflerinin pıhtılaşma süreleri benzerdi; ancak ABS/PVA nanoliflerinin pıhtılaşma süresi daha kısaydı. Bulgulara göre, adrenalin/PVA nanolifleri en uzun pıhtılaşma süresine sahiptir ve bu süre 4.088

saniyeydi. Öte yandan, ABS/PVA nanolifleri en kısa pıhtılaşma süresine sahipti ve bu süre 3.819 saniyeydi. İyi bir hemostat, *in vitro* uygulamalarda yara bölgesine uygulandıktan sonra 2 dakika içinde kanamayı durdurabilmeli, karıştırma veya hazırlama gerektirmemeli ve yaralı bölgelere basitçe uygulanabilmelidir. Bu çalışmada elde edilen hemostatik nanoliflerin saniyeler içinde pıhtı oluşturabilme yeteneği gösterilmiştir. Geliştirilen nanolifler, sadece halk sağlığı açısından değil, aynı zamanda hayatta kalma süreçlerine güçlü bir katkı sağlayacaktır.

1. Introduction

Hemostatics are a type of drugs that promote hemostasis, which is the natural process of forming clots to prevent or stop bleeding [1]. The hemostasis process involves vasoconstriction, platelet plug formation, and blood coagulation [2]. Hemostatic agents can be classified into two main categories: topical and systemic. Topical hemostatics are administered directly at the site of bleeding, where they function by either forming a physical barrier, initiating the coagulation process, or improving platelet aggregation. Some illustrations of topical hemostatics comprise collagen, gelatin, cellulose, fibrin sealants, and thrombin [3]. Systemic hemostatics, on the other hand, are given intravenously and function by increasing clotting factor levels, inhibiting fibrinolysis, or boosting platelet function. Examples of systemic hemostatics include tranexamic acid, aminocaproic acid, desmopressin, and recombinant factor VIIa [3]. In situations where there is a high risk of severe bleeding, hemostatics are essential in various health fields. Military medicine is one field where hemostatics can be utilized to treat combat casualties with traumatic hemorrhage. Up to 90% of potentially survivable deaths among soldiers in modern warfare are due to hemorrhage. Hence, the use of hemostatics can considerably improve survival rates and reduce morbidity among injured soldiers. Soldiers can self-administer these hemostatics at the injury site, during evacuation, or at the hospital, or they can be administered by combat medics. Some of the hemostatics evaluated or used by the military include QuikClot®, HemCon®, WoundStat®, Celox®, Combat Gauze, and TXA. However, hemostatics pose several limitations and challenges, such as cost, availability, safety, efficacy, applicability, and compatibility with various wound types. Therefore, further research and development are necessary to optimize the use of hemostatics.

Hemorrhage, especially from noncompressible areas like the splanchnic and junctional areas, continues to be the primary cause of avoidable fatalities on the battlefield [4, 5]. In the United States, during conflicts in Iraq and Afghanistan a staggering 90% of combat casualties succumbed to their injuries before reaching surgical facilities. Among these casualties, Hemorrhage was responsible for about 90% of potentially survivable fatalities, with 67% occurring in truncal areas, 19% in junctional areas, and 14% in extremities [5, 6]. It is worth mentioning that a considerable proportion of in-hospital fatalities occur during the first hour of admission [7]. Hence, the development and deployment of effective hemostatic agents for use both in the prehospital and early in-hospital stages are of paramount importance.

Electrospinning is a cost-effective and straightforward method that involves four essential components: 1. a high-voltage power source, 2. a spinneret, 3. a collector, and 4. a

feeding system. Electrospun nanofibers have been widely employed in the biomedical sector, with significant applications in fields such as tissue engineering [8] and wound dressings [9]. In times of conflict and crises, severe bleeding and wound infections resulting from tissue injuries are primary contributors to casualties. Hence, the development of hemostatic agents for early use in both prehospital and early in-hospital settings is of paramount importance. There is a growing interest in harnessing nanofibers to achieve swift hemostasis, and nanofibers tailored for this purpose have attracted considerable attention. These nanofibers possess an extensive surface area and substantial porosity, enabling them to adhere tightly to the bleeding spot. Additionally, they facilitate platelet attachment and activation, expediting the local formation of blood clots [10].

Archana et al. [11] successfully developed a chitosan-PVP-Ag₂O hemostatic membrane. The incorporation of Polyvinylpyrrolidone (PVP) not only enhanced the strength and mechanical characteristics of the hemostatic membrane but also led to cost reduction. Additionally, the effective combination of nano silver's strong antibacterial properties with chitosan's inherent antibacterial qualities resulted in a dual antibacterial effect that outperformed other materials used for healing purposes. In the study conducted by Lu and colleagues [12], they integrated silver/zinc oxide into a chitosan sponge, which was prepared through lyophilization and intended for use in hemostasis. This composite exhibited notable porosity and swelling characteristics. The results of animal experiments indicated that this composite dressing not only improved coagulation and antibacterial efficacy but also displayed minimal toxicity. Furthermore, the dressing was found to facilitate the process of re-epithelialization and the deposition of collagen. Fatahian et al. [13] produced a hemostatic wound dressing by mixing TXA with PVA. It has investigated blood coagulation properties. According to the study results, PVA-TXA dressings showed acceptable blood clotting capacity.

Epinephrine, commonly known as adrenaline, is a catecholamine hormone with a wide range of functions in the human body's physiology. It is released into the bloodstream when the sympathetic nervous system is activated [14]. Initially, it was thought that adrenaline primarily affected hemostasis by constricting blood vessels [15]. However, subsequent research has revealed that human platelets possess α_2 A-adrenergic receptors (AR) that are associated with G_z proteins, a subtype of G_i protein [16-18]. When adrenaline binds to these platelet α_2 -AR receptors, it inhibits the activity of adenylate cyclase (AC), resulting in a decrease in cytosolic cyclic AMP concentration. This reduction in cyclic AMP levels, which acts as a negative regulator of platelet

activation, suggests that adrenaline may, in fact, facilitate the platelet activation process and thus contribute to the formation of blood clots (thrombus) [19, 20].

Tranexamic acid is a synthetic compound derived from lysine, and its primary mode of action involves antifibrinolytic effects. It achieves this by obstructing the lysine binding sites found on plasminogen molecules, thereby preventing the interaction between plasminogen, formed plasmin, and fibrin. Consequently, this inhibition of plasminogen activation leads to the stabilization of the pre-existing fibrin network created during the secondary hemostasis process [21]. ABS is an herbal extract that has been traditionally used in Turkey and Bosnia and Herzegovina to treat bleeding. ABS has antibacterial, antiseptic, and antimicrobial properties. Laboratory studies conducted in controlled environments have demonstrated that ABS exhibits effectiveness against a broad spectrum of bacteria, including both Gram-positive and Gram-negative types [22]. It has also displayed efficacy against foodborne pathogens [23], drug-resistant nosocomial (hospital-acquired) pathogens [24], and drug-resistant strains of Tuberculosis. These antimicrobial properties of Ankaferd can be attributed to its chemical composition and ingredients.

The objective of this study was to manufacture a nonwoven nanofiber material suitable for use as a hemostatic wound dressing. In this study, nanofibers possessing hemostatic properties were produced through the electrospinning method, employing ADR, TXA, and ABS as hemostatic agents in combination with PVA polymer. The investigation involved the analysis of the morphology and chemical bonding structures of these hemostatic nanofibers, and the assessment of their hemostatic efficacy.

2. Method and Materials

2.1. Materials

PVA (125,000 MW, 99% hydrolyzed) used in the production of nanofibers, and Glutaraldehyde (GA) (50% aqueous solution) was purchased from Sigma-Aldrich Co. (St. Louis, U.S.A.). ABS was purchased from Trend Teknoloji İlaç A.Ş. (Istanbul, Turkey). TXA, ADR, and medical sterile gauzes were purchased from commercial sources. All reagents were analytical grade and used as received.

2.2. Solution Preparation

PVA solution (12 %, w/w) was prepared by dissolving PVA in pure water under stirring gently at 100 °C until completely dissolved then cooled to room temperature. ADR/PVA, solution was prepared by adding ADR to PVA solution at 50% of the total polymer solution weight. The obtained solution was stirred with a magnetic stirrer at 200 rpm for 2 hours. The same process was done for the TXA and ABS solutions. To improve the spinnability of the ABS/PVA solution 0.01 g of NaCl was added to the PVA solution (12 %, w/w).

2.3. Fabrication of Hemostatic Membranes

The spinning solution was prepared and then moved to a 5 mL syringe with a 20 G stainless steel needle. The distance between the needle and the collector, which was covered with aluminum foil and sterile gauze, was adjusted to 15 cm. The electrospinning process was carried out at room temperature, hemostatic nanofibers were produced at a steady flow rate of 0.8 ml/h and 14 kV. The resulting electrospun fibers were stored for future use and labeled according to the hemostatic agents employed: PVA, ADR/PVA, TXA/PVA, and ABS/PVA.

2.4. Binding Nanofiber Samples to Fabric

Since nanofiber materials are sensitive, they are not expected to have mechanical strength, and therefore mechanical strength tests were not performed. The purpose of combining these materials with nonwoven textile surfaces is to obtain mechanically durable nanofibers. The hemostatic nanofibers obtained within the study were attached to fabric samples using an ultrasonic binding process. The ultrasonic binding procedure was carried out at a speed of 5 m/min at a frequency of 20 kHz. Table 1 summarizes the nanofiber samples utilized in the binding procedures, binding techniques, and fabric properties acquired from the Mogul company.

2.5. Characterization

2.5.1. FESEM

The morphology of the nanofiber samples were analyzed by Field Emission Scanning Electron Microscopes (FESEM). Each sample was coated with a conductive surface gold-palladium (Quorum Q150R). All FESEM images (SUPRA 40VP, Carl Zeiss, Germany) were obtained at 20 kV. Image J software was used to calculate the average diameters of the nanofibers.

2.5.2. FT-IR

The chemical bond structures of hemostatic nanofibers were analyzed by Fourier Transform Infrared Spectrophotometer (IS50 FT-IR, Thermo Scientific, USA) containing Diamond ATR crystal. FT-IR spectra were recorded between 450 and 4000 cm^{-1} with a resolution of 1 cm^{-1} .

2.5.3. Nanofiber samples swelling rate

Since the obtained samples are instantly soluble in water, crosslinking of the samples with GA vapor was carried out. In this context, PVA, ADR/PVA, TXA/PVA and ABS/PVA nanofibers were exposed to GA vapor in a closed container for 24 hours at room temperature. Then the swelling and weight loss percentages of the nanofibers were calculated by soaking them in distilled water for 24 hours, then drying and weighing them. In the first step, nanofiber samples of similar sizes were weighed and noted. In the second step, the nanofiber samples were soaked in distilled water for 24 hours. After that, the samples were taken out, placed on filter paper briefly to eliminate any excess surface water, and then weighed.

Table 1. Nanofiber samples, binding methods and fabrics used in the binding processes

| NO | Used fabric layers | Used Nanofiber Sample | Binding Method | Strength of Materials MD* (N/5 cm) | Strength of Materials CD* (N/5 cm) |
|----|-----------------------------------|-----------------------|----------------|------------------------------------|------------------------------------|
| 1 | A4 40 gsm spunlace flat Bio-based | PVA | Ultrasonic | 95 | 110 |
| 2 | A4 40 gsm spunlace flat Bio-based | ADR/PVA | Ultrasonic | 95 | 110 |
| 3 | A4 40 gsm spunlace flat Bio-based | TXA/PVA | Ultrasonic | 95 | 110 |
| 4 | A4 40 gsm spunlace flat Bio-based | ABS/PVA | Ultrasonic | 95 | 110 |

* MD = Machine Direction, CD = Cross Direction

In the third step, the samples were dried at room temperature for 24 hours and weighed again. The measurements were taken three times. In addition, the average and standard deviation values were calculated. The percentage swelling was calculated according to equation 1 and weight loss was calculated according to equation 2.

$$\text{Swelling Percentage (\%)} = \frac{M - M_d}{M_d} \times 100 \quad (1)$$

and

$$\text{Weight Loss (\%)} = \frac{M_i - M_d}{M_i} \times 100 \quad (2)$$

M_i: Initial weight, M: Swollen weight, M_d: Dry weight

2.5.4. Determination of hemostatic nanofibers hemostatic efficiency

Clotting time was calculated using fresh human blood drawn from a volunteer. The drop measurement approach was used in this context, where a drop of blood was deposited on the hemostatic nanofiber samples and the clot formation time was evaluated. For each nanofiber sample, the measurement technique was performed ten times, and the average clotting time was determined. The study was approved by Pamukkale University Noninterventional Clinical Research Ethical Committee (Decision no: 07, Date: 18.04.2023).

3. Results

3.1. FESEM

The morphology of PVA, ADR/PVA, TXA/PVA, and ABS/PVA was investigated using FESEM images (Figure 1). The average diameter of 30 random fibers was calculated after measuring their diameters. This procedure was followed for all samples. Table 2 shows the minimum, maximum, and the average sizes of the observed nanofibers.

Table 2. Minimum, maximum, and average diameters of hemostatic nanofibers

| Sample | Minimum Diameter (nm) | Maximum Diameter (nm) | Average Diameter (nm) | Standard Deviation |
|---------|-----------------------|-----------------------|-----------------------|--------------------|
| PVA | 390 | 1079 | 605.933 | 0.1870 |
| ADR/PVA | 168 | 403 | 251.667 | 0.0514 |
| TXA/PVA | 151 | 512 | 226.867 | 0.0938 |
| ABS/PVA | 163 | 293 | 226.867 | 0.0382 |

3.2. FT-IR

The chemical structures of PVA, ADR/PVA, TXA/PVA and ABS/PVA were characterized using FT-IR spectroscopy. FT-IR spectra of hemostatic nanofiber samples are given in Figure 2.

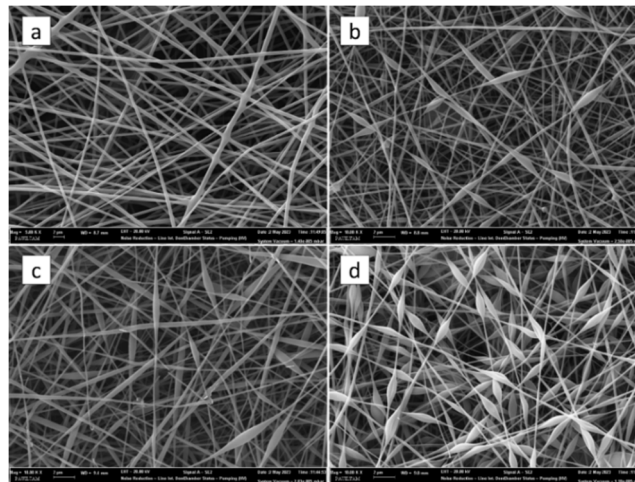


Figure 1. FESEM images of hemostatic nanofibers at 10000X magnification (Scale Bar: 2 μm). a) PVA, b) ADR/PVA, c) TXA/PVA, d) ABS/PVA.

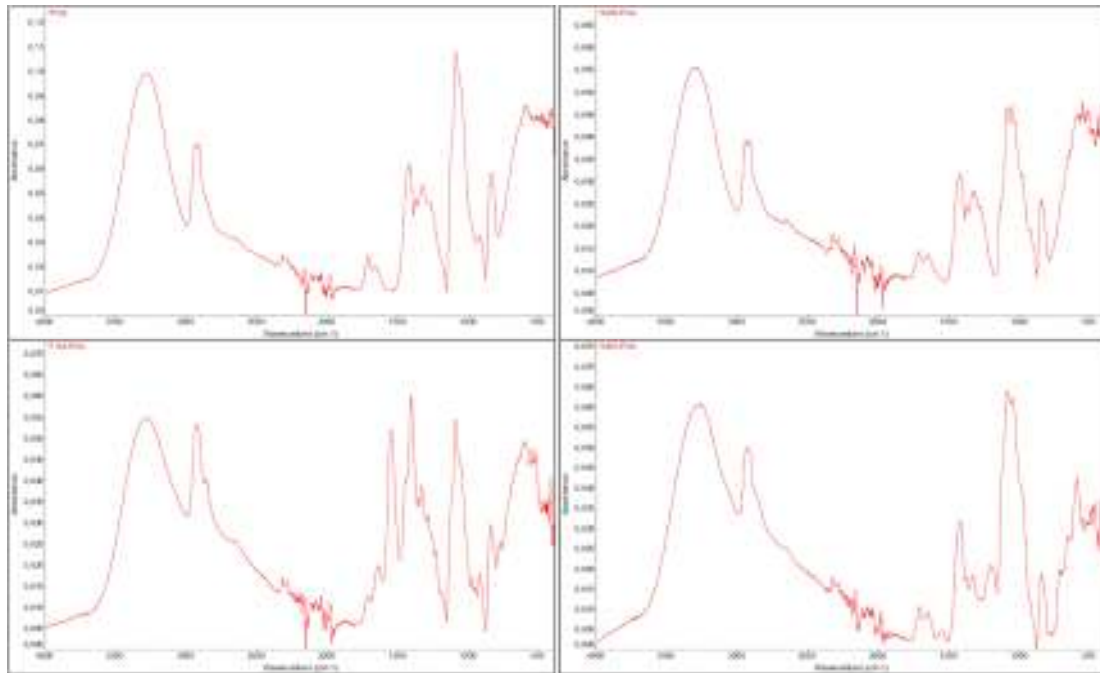


Figure 2. FT-IR spectra of a) PVA, b) ADR/PVA, c) TXA/PVA and d) ABS/PVA nanofiber samples

3.3. Nanofiber Samples Swelling Rate

Figure 3 Shows the swelling ratio and weight loss of the hemostatic nanofiber samples. The average and standard deviation of the starting weight, swollen weight, and dry weight are presented in Table 3.

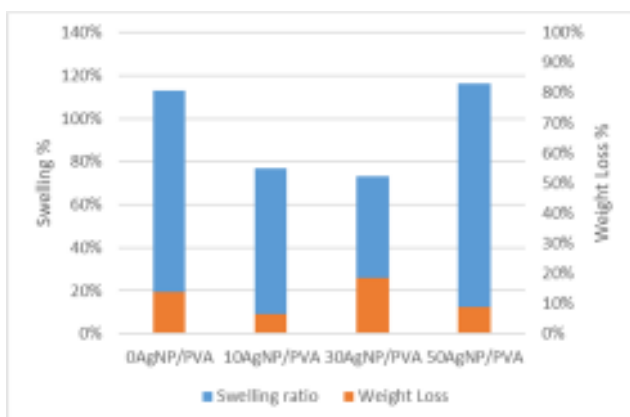


Table 3. The average and standard deviation of the starting weight, swollen weight, and dry weight of nanofibers samples

| Sample | Initial weight (g) | | Swollen weight (g) | | Dry weight (g) | |
|---------|--------------------|--------------------|--------------------|--------------------|----------------|--------------------|
| | Average | Standard Deviation | Average | Standard Deviation | Average | Standard Deviation |
| PVA | 0.00493 | 0.00006 | 0.00923 | 0.00045 | 0.00433 | 0.00015 |
| ADR/PVA | 0.00277 | 0.00015 | 0.00460 | 0.00030 | 0.00260 | 0.00010 |
| TXA/PVA | 0.00383 | 0.00015 | 0.00560 | 0.00040 | 0.00323 | 0.00006 |
| ABS/PVA | 0.00537 | 0.00021 | 0.01067 | 0.00115 | 0.00493 | 0.00012 |

Figure 3. Swelling ratio and weight loss of PVA, ADR/PVA, TXA/PVA and ABS/PVA nanofibers

3.4. Determination of Hemostatic Nanofibers Hemostatic Efficiency

According to the measurements, the clotting times of ADR/PVA and TXA/PVA nanofibers were similar, yet ABS/PVA had a lower clotting time. Table 4 shows the results of the hemostatic activity measuring experiments.

Table 4. Hemostatic activity measurement test results

| Sample | Minimum clotting time (sec) | Maximum clotting time (sec) | Average clotting time (sec) |
|---------|-----------------------------|-----------------------------|-----------------------------|
| PVA | No clotting was observed | No clotting was observed | No clotting was observed |
| ADR/PVA | 2 | 6 | 4.088 |
| TXA/PVA | 3 | 8 | 4.602 |
| ABS/PVA | 2 | 6 | 3.819 |

4. Discussion

PVA polymer is a hydrophilic, semi-crystalline, semi-crystalline, hydrophilic polymer with high thermal and chemical stability, is generally regarded as safe (GRAS), is non-toxic, and has good thermal and chemical stability, according to the literature. It is extensively utilized in electrospinning systems because of its great biocompatibility and inexpensive cost [25, 26]. As a result, PVA polymer was chosen for the fabrication of hemostatic nanofibers.

According to the FESEM images, beaded fibers started to form with the addition of ADR, TXA and ABS. ABS/PVA and TXA/PVA nanofibers had the same average nanofiber diameter, yet ABS/PVA had more beaded morphology than TXA/PVA.

Figure 2a shows the FTIR spectrum of PVA nanofibers. The absorption bands seen in the spectrum of PVA nanofibers are as follows: The peak at 3272 cm^{-1} refers to the stretching vibration due to the O-H group. The 2913 cm^{-1} and 1332 cm^{-1} bands show symmetric stretching vibration of $-\text{CH}_2$ group, 1710 cm^{-1} and 1649 cm^{-1} bands show C=O stretching vibration, 1420 cm^{-1} band shows CH_2 bending vibration, 1086 cm^{-1} band shows C-O stretching vibration, and 839 cm^{-1} band shows C-C stretching vibration. These results agree with previous studies in literature [27-33].

Figure 2b shows the FTIR spectrum of ADR/PVA nanofibers. The peak observed at 3400 cm^{-1} in the spectrum can be ascribed to the N-H bonds present in epinephrine. Furthermore, the presence of ADR (presumably adrenaline) appears to enhance the vibration at 3282 cm^{-1} , which corresponds to the O-H bond. It's worth noting that the absorbance in the 3282 cm^{-1} region may also be attributed to the benzene structure present in epinephrine [34, 35].

Figure 2c shows the FTIR spectrum of TXA/PVA nanofibers. In the PVA spectrum, the primary vibrational modes arise from the hydroxyl and acetate groups. To be more specific, the peak observed at 3296 cm^{-1} corresponds to the stretching of O-H bonds, while the peak at 2923 cm^{-1} results from the asymmetric stretching vibration of alkyl groups' C-H bonds. On the other hand, in the TXA spectrum, we observe peaks at 1450 cm^{-1} (methylene group), 1532 cm^{-1} (indicative of the presence of carbonyl groups), and 2858 cm^{-1} (associated with C-H stretching vibrations) [36]. Figure 2d shows the FTIR spectrum of ABS/PVA nanofibers. In the interpretation of the spectrum of ABS/PVA samples, the FTIR peaks formed by ABS content [37] were analyzed. The peak at 2937 cm^{-1} can be attributed to the aliphatic $\text{CH}_3 - \text{CH}_2$ stretching vibration [38]. 2918 cm^{-1} can be attributed to the stretching vibration, 1333 cm^{-1} can be attributed to NO_2 , and 1085 cm^{-1} peak can be attributed to C-F stretching vibration [39]. The characteristic indications of *Thymus Vulgaris* include the bending of O-H groups within the range of $1340\text{-}1255\text{ cm}^{-1}$, the absorption peak associated with C-OH stretching at 1053 cm^{-1} , and peaks attributed to the out-of-plane bending of O-H groups in the region between $736\text{-}590\text{ cm}^{-1}$ [40]. These peaks overlap with the peaks formed by *Timus vulgaris*, *Glycyrrhiza glabra*, *Vitis vinifera*, *Alpinia officinarum* and *Urtica dioica* in ABS [40-48].

The swelling characteristics of PVA, ADR/PVA, TXA/PVA,

and ABS/PVA samples were examined by immersing the nanofiber membrane in distilled water for a 24-hour period. TXA/PVA displayed the lowest swelling ratio, at 73%, while ABS/PVA exhibited the highest swelling ratio, reaching 118%. The reduction in PVA concentration due to an increase in the concentration of hemostatic agents led to the production of thinner fibers. Notably, thinner fibers demonstrated reduced swelling properties. TXA/PVA nanofibers showed a greater weight loss compared to PVA, ADR/PVA, and ABS/PVA nanofibers. Overall, all the samples underwent successful crosslinking with glutaraldehyde vapor, and no significant weight loss was observed.

Hemostasis is a mechanism that prevents excessive blood loss after vascular injury and keeps the physiological process that regulates blood fluidity in check while also preventing blood from coagulating. Primary and secondary hemostasis are two types of hemostasis. Primary hemostasis takes about 4 to 7 minutes and deals with the body's initial reactions to the injury [49,50]. Mucocutaneous bleeding (petechiae, epistaxis, gingival bleeding, hematuria, and menorrhagia) and severe bleeding after trauma or incisions are frequent in diseases that affect primary hemostasis. Local control of bleeding is essential and beneficial in primary hemostasis disorders. This can be achieved by exerting pressure on the bleeding area and applying local hemostatic agents like tranexamic acid, adrenalin, and ABS [51,52].

Since nanofiber materials are sensitive, they are not expected to have mechanical strength. The hemostatic nanofibers were adhered to nonwoven textiles thus mechanically durable nanofiber surfaces were obtained. The ultrasonic binding process preserved the suppleness of the samples. However, the layers can separate if they are forced. The nonwoven fabrics did not affect the hemostatic activity of the nanofibers since they were adhered only to one side. The hemostatic activity of the obtained nanofibers was evaluated. In this context, tests were performed using the drop measurement technique. According to the results ADR/PVA had the longest clotting time with 4.088 second while ABS/PVA had the shortest clotting time with 3.819 second.

There are currently various hemostatic agents available for achieving rapid hemostasis. Adrenaline, an adrenergic substance, can be applied directly to the bleeding site to assist in controlling bleeding. When administered in low doses, adrenaline activates the coagulation system and may help reduce bleeding during surgery and in the immediate postoperative period. Adrenaline works by stimulating receptors on the mucous membrane, leading to local vasoconstriction (53). Another hemostatic option is ABS, which is a standardized mixture containing five different plant extracts: *Vitis vinifera*, *Thymus vulgaris*, *Glycyrrhiza glabra*, *Alpinia officinarum*, and *Urtica dioica*. ABS achieves its hemostatic effect by creating an encapsulated protein network that promotes the essential physiological aggregation of erythrocytes, all without interfering with the normal coagulation processes of individuals. ABS is used effectively in medical settings on patients with primary and secondary hemorrhagic diathesis [53]. In a study done by Badovinac et al., TXA was found to be just as effective as adrenaline in managing severe endobronchial hemorrhage [54]. In an animal experiment, it was shown that ABS stopped

epistaxis more quickly than gelatin foam, adrenaline + lidocaine, and serum physiologic as negative control [55]. In accordance with these results, our study found that ADR/PVA and TXA/PVA nanofibers had nearly similar clotting times, but ABS/PVA had a quicker clotting effect.

Nanofibers have shown great promise in the field of hemostasis due to their structural similarity to fibrin clots. Extensive research has been conducted over the past two decades to develop various manufacturing processes for the creation of nanofibrous materials that can be used for both external and intracavitary hemostatic control. The ideal hemostat for in vivo applications should clot blood quickly, be biocompatible and biodegradable, not carry the risk of bacterial or viral contamination, and promote wound healing. Furthermore, good hemostats should stop bleeding in in vitro applications within 2 minutes after administration to the wound site, should not require mixing or prior preparation, and should be simple to administer to injured regions [56]. The hemostatic nanofibers obtained in this study showed the ability to form clots within seconds. The behavior of the obtained hemostatic nanofibers under different conditions needs to be investigated. These additional tests are planned for future research. The developed nanofibers will have a strong added value effect not only in terms of public health but also in survival processes.

Nanofibers have shown great promise in the field of hemostasis due to their structural similarity to fibrin clots. Extensive research has been conducted over the past two decades to develop various manufacturing processes for the creation of nanofibrous materials that can be used for both external and intracavitary hemostatic control. The ideal hemostat for in vivo applications should clot blood quickly, be biocompatible and biodegradable, not carry the risk of bacterial or viral contamination, and promote wound healing. Furthermore, good hemostats should stop bleeding in in vitro applications within 2 minutes after administration to the wound site, should not require mixing or prior preparation, and should be simple to administer to injured regions [56]. The hemostatic nanofibers obtained in this study showed the ability to form clots within seconds. The behavior of the obtained hemostatic nanofibers under different conditions needs to be investigated. Additional optimization studies are planned for future research. The developed nanofibers will have a strong added value effect not only in terms of public health but also in survival processes.

Conflict of Interest

No conflict of interest was declared by the authors.

Financial Disclosure

The authors declared that this study received no financial support.

References

[1] Çolak, S., Altan, A., Akbulut, N. (2018). Lokal Hemostatik Ajanlar. Uluslararası Dış Hekimliği Bilimleri Dergisi, (3), 147-152.

- [2] Sierra, C., Moreno, M. U., & García-Ruiz, J. C. (2022). The physiology of hemostasis. *Blood Coagulation & Fibrinolysis*, 33(S1), S1–S2. <https://doi.org/10.1097/mbc.0000000000001099>
- [3] Sruthi, S.M., (2021, August 4). How do hemostatics work? - uses, side effects, drug names. RxList. https://www.rxlist.com/how_do_hemostatics_work/drug-class.htm
- [4] Stannard, A., Morrison, J. J., Scott, D., Ivatury, R. A., Ross, J. D., & Rasmussen, T. E. (2013). The epidemiology of noncompressible torso hemorrhage in the wars in Iraq and Afghanistan. *The Journal of Trauma and Acute Care Surgery*, 74(3), 830–834. <https://doi.org/10.1097/ta.0b013e31827a3704>
- [5] Eastridge, B. J., Hardin, M. O., Cantrell, J. A., Oetjen-Gerdes, L., Zubko, T., Mallak, C. T., Wade, C. E., Simmons, J. W., Mace, J. E., Mabry, R., Bolenbaucher, R., & Blackbourne, L. H. (2011). Died of Wounds on the Battlefield: Causation and implications for Improving Combat Casualty care. *Journal of Trauma-injury Infection and Critical Care*, 71(1), S4–S8. <https://doi.org/10.1097/ta.0b013e318221147b>
- [6] Eastridge, B. J., Mabry, R., Seguin, P., Cantrell, J. A., Tops, T., Uribe, P., Mallett, O., Zubko, T., Oetjen-Gerdes, L., Rasmussen, T. E., Butler, F. K., Kotwal, R. S., Holcomb, J. B., Wade, C. E., Champion, H. R., Lawnick, M., Moores, L. E., & Blackbourne, L. H. (2012). Death on the battlefield (2001–2011). *The Journal of Trauma and Acute Care Surgery*, 73(6), S431–S437. <https://doi.org/10.1097/ta.0b013e3182755dcc>
- [7] Martin, M. J., Oh, J. S., Currier, H., Tai, N., Beekley, A. C., Eckert, M. J., & Holcomb, J. B. (2009). An analysis of In-Hospital deaths at a modern combat support Hospital. *Journal of Trauma-injury Infection and Critical Care*, 66(4), S51–S61. <https://doi.org/10.1097/ta.0b013e31819d86ad>
- [8] Bakhsheshi-Rad, H. R., Ismail, A. F., Aziz, M., Hadisi, Z., Omidi, M., & Chen, D. (2019). Antibacterial activity and corrosion resistance of Ta2O5 thin film and electrospun PCL/MgO-Ag nanofiber coatings on biodegradable Mg alloy implants. *Ceramics International*, 45(9), 11883–11892. <https://doi.org/10.1016/j.ceramint.2019.03.071>
- [9] Balusamy, B., Senthamizhan, A. & Uyar, T. (2020). Electrospun Nanofibers for Wound Dressing and Tissue Engineering Applications. *Hacetatepe Journal of Biology and Chemistry, The 100 Year of Polymers*, 459-481. DOI: 10.15671/hjbc.789186
- [10] Zhao, Y., Qiu, Y., Wang, H., Chen, Y., Jin, S., & Chen, S. (2016). Preparation of nanofibers with renewable polymers and their application in wound dressing. *International Journal of Polymer Science*, 2016.
- [11] Archana, D., Singh, B. K., Dutta, J., & Dutta, P. K. (2015). Chitosan-PVP-nano silver oxide wound dressing: in vitro and in vivo evaluation. *International journal of biological macromolecules*, 73, 49-57.
- [12] Lu, Z., Gao, J., He, Q., Wu, J., Liang, D., Yang, H., & Chen, R. (2017). Enhanced antibacterial and wound healing activities of microporous chitosan-Ag/ZnO composite dressing. *Carbohydrate polymers*, 156, 460-469.
- [13] Fatahian, R., Mirjalili, M., Khajavi, R., Rahimi, M. K., & Nasirizadeh, N. (2020). Fabrication of antibacterial and hemostatic electrospun PVA nanofibers for wound healing. *SN Applied Sciences*, 2, 1-7.
- [14] Goldstein, D. S. (2010). Catecholamines

101. Clinical Autonomic Research, 20, 331-352.
- [15] von Känel, R. (2015). Acute mental stress and hemostasis: when physiology becomes vascular harm. *Thrombosis research*, 135, S52-S55.
- [16] Mukherjee, A. (1981). Characterization of α_2 -adrenergic receptors in human platelets by binding of a radioactive ligand [3H] yohimbine. *Biochimica et Biophysica Acta (BBA)-General Subjects*, 676(2), 148-154.
- [17] Yang, J., Wu, J., Kowalska, M. A., Dalvi, A., Prévost, N., O'Brien, P. J., Manning, D. R., Poncz, M., Lucki, I., Blendy, J. A., & Brass, L. F. (2000). Loss of signaling through the G protein, Gz, results in abnormal platelet activation and altered responses to psychoactive drugs. *Proceedings of the National Academy of Sciences of the United States of America*, 97(18), 9984-9989. <https://doi.org/10.1073/pnas.180194597>
- [18] Woulfe, D. S., Jiang, H., Mortensen, R. M., Yang, J., & Brass, L. F. (2002). Activation of RAP1B by GI family members in platelets. *Journal of Biological Chemistry*, 277(26), 23382-23390. <https://doi.org/10.1074/jbc.m202212200>
- [19] Sachs, U. J., & Nieswandt, B. (2007). In vivo thrombus formation in murine models. *Circulation Research*, 100(7), 979-991. <https://doi.org/10.1161/01.res.0000261936.85776.5f>
- [20] Stalker, T. J., Newman, D. K., Ma, P., Wannemacher, K. M., & Brass, L. F. (2012). Platelet signaling. In *Handbook of experimental pharmacology* (pp. 59-85). https://doi.org/10.1007/978-3-642-29423-5_3
- [21] Cai, J., Ribkoff, J., Olson, S. R., Raghunathan, V., Al-Samkari, H., DeLoughery, T. G., & Shatzel, J. J. (2019). The many roles of tranexamic acid: An overview of the clinical indications for TXA in medical and surgical patients. *European Journal of Haematology*, 104(2), 79-87. <https://doi.org/10.1111/ejh.13348>
- [22] Akkoç, N., Akçelik, M., Haznedaroğlu, İ. C., Göker, H., Turğut, M., Aksu, S., Kirazlı, Ş., & Firat, H. C. (2009). In vitro anti-bacterial activities of Ankaferd medicinal plant extract. *Türkiye Klinikleri Tıp Bilimleri Dergisi*, 29(2), 410-415.
- [23] Koluman, A., Akar, N., & Haznedaroğlu, İ. C. (2017). Antibacterial Activities of Ankaferd Hemostat (ABS) on Shiga Toxin-Producing *Escherichia coli* and other Pathogens Significant in Foodborne Diseases. *Turkish Journal of Hematology*, 34(1), 93-98. <https://doi.org/10.4274/tjh.2015.0073>
- [24] Sarıbaş, Z., Şener, B., Haznedaroğlu, İ. C., Hasçelik, G., Kirazlı, Ş., & Göker, H. (2010). Antimicrobial activity of Ankaferd Blood Stopper® against nosocomial bacterial pathogens. *Open Medicine*, 5(2), 198-202. <https://doi.org/10.2478/s11536-009-0140-4>
- [25] Koski, A., Yim, K., & Shivkumar, S. (2004). Effect of molecular weight on fibrous PVA produced by electrospinning. *Materials Letters*, 58(3-4), 493-497. [https://doi.org/10.1016/s0167-577x\(03\)00532-9](https://doi.org/10.1016/s0167-577x(03)00532-9)
- [26] McFarland, L. V. (2006). Meta-Analysis of Probiotics for the Prevention of Antibiotic Associated Diarrhea and the Treatment of *Clostridium difficile* Disease. *The American Journal of Gastroenterology*, 101(4), 812-822. <https://doi.org/10.1111/j.1572-0241.2006.00465.x>
- [27] El Bahy, G. S., El-Sayed, E. S. M., Mahmoud, A. A., & Gweily, N. M. (2012). Preparation and characterization of poly vinyl alcohol/gelatin blends. *J. Appl. Sci. Res*, 8(7), 3544-3551.
- [28] Kharazmi, A., Faraji, N., Hussin, R. M., Saion, E., Yunus, W. M. M., & Behzad, K. (2015). Structural, optical, opto-thermal and thermal properties of ZnS-PVA nanofluids synthesized through a radiolytic approach. *Beilstein Journal of Nanotechnology*, 6, 529-536. <https://doi.org/10.3762/bjnano.6.55>
- [29] Abureesh, M. A., Oladipo, A. A., & Gazi, M. (2016). Facile synthesis of glucose-sensitive chitosan-poly(vinyl alcohol) hydrogel: Drug release optimization and swelling properties. *International Journal of Biological Macromolecules*, 90, 75-80. <https://doi.org/10.1016/j.ijbiomac.2015.10.001>
- [30] Li, T., Yan, M., Zhong, Y., Ren, H., Lou, C., Huang, S., & Lin, J. (2019). Processing and characterizations of rotary linear needleless electrospun polyvinyl alcohol(PVA)/Chitosan(CS)/Graphene(Gr) nanofibrous membranes. *Journal of Materials Research and Technology*, 8(6), 5124-5132. <https://doi.org/10.1016/j.jmrt.2019.08.035>
- [31] Zhuang, J., Li, M., Pu, Y., Ragauskas, A. J., & Yoo, C. G. (2020). Observation of potential contaminants in processed biomass using Fourier Transform infrared spectroscopy. *Applied Sciences*, 10(12), 4345. <https://doi.org/10.3390/app10124345>
- [32] Ge, J. C., Wu, G., Yoon, S. K., Kim, M. S., & Choi, N. J. (2021). Study on the preparation and lipophilic properties of polyvinyl alcohol (PVA) nanofiber membranes via green electrospinning. *Nanomaterials*, 11(10), 2514. <https://doi.org/10.3390/nano11102514>
- [33] Web Anonymous 1., Chapter 4: Fourier Transform Infrared Spectroscopy (FTIR). [Online]. Available: http://studentsrepo.um.edu.my/6086/11/Chapter_4_-_Section_1.pdf.
- [34] Wang, S. F., Du, D., & Zou, Q. C. (2002). Electrochemical behavior of epinephrine at L-cysteine self-assembled monolayers modified gold electrode. *Talanta*, 57(4), 687-692.
- [35] Lee, F., Lee, D., Lee, T., Chen, J., Wu, R., Liu, K., & Liu, S. (2017). Fabrication of Multi-Layered Lidocaine and Epinephrine-Eluting PLGA/Collagen Nanofibers: In Vitro and In Vivo Study. *Polymers*, 9(12), 416. <https://doi.org/10.3390/polym9090416>
- [36] Sezer, Ü. A., Koçer, Z., Aru, B., Demirel, G. Y., Gülmez, M., Aktekin, A., Özkara, S., & Sezer, S. (2016). Combination of gelatin and tranexamic acid offers improved haemostasis and safe use on internal hemorrhage control. *RSC Advances*, 6(97), 95189-95198. <https://doi.org/10.1039/c6ra16790j>
- [37] Göker, H., Haznedaroğlu, İ. C., Ercetin, S., Kirazlı, Ş., Akman, Ü., Öztürk, Y., & Firat, H. C. (2008). Haemostatic actions of the folkloric medicinal plant extract Ankaferd blood Stopper®. *Journal of International Medical Research*, 36(1), 163-170. <https://doi.org/10.1177/147323000803600121>
- [38] Yang, J., Wang, K., Yu, D., Yang, Y., Bligh, S. W. A., & Williams, G. R. (2020). Electrospun Janus nanofibers loaded with a drug and inorganic nanoparticles as an effective antibacterial wound dressing. *Materials Science and Engineering: C*, 111, 110805. <https://doi.org/10.1016/j.msec.2020.110805>
- [39] Al-Tameme, H. J., Hameed, I. H., Idan, S. A., & Hadi, M. Y. (2015). Biochemical analysis of *Origanum vulgare* seeds by fourier-transform infrared (FT-IR) spectroscopy and gas chromatography-mass spectrometry (GC-MS). *Journal of Pharmacognosy and Phytotherapy*,

- 7(9), 221–237. <https://doi.org/10.5897/jpp2015.0362>
- [40] Catauro, M., Bollino, F., Tranquillo, E., Sapio, L., Illiano, M., Caiafa, I., & Naviglio, S. (2017). Chemical analysis and anti-proliferative activity of Campania Thymus Vulgaris essential oil. *Journal of Essential Oil Research*, 29(6), 461–470. <https://doi.org/10.1080/10412905.2017.1351405>
- [41] Demiralp, D. Ö. (2013). The Fourier Transform Infrared (FTIR) spectroscopic and mass spectrometric metabolomics studies of Ankaferd hemostat. *International Journal of Hematology and Oncology*, 23(3), 171–177. <https://doi.org/10.4999/uhod.12059>
- [42] Al-Tameme, H. J., Hadi, M. Y., & Hameed, I. H. (2015). Phytochemical analysis of Urtica dioica leaves by fourier-transform infrared spectroscopy and gas chromatography-mass spectrometry. *Journal of Pharmacognosy and Phytotherapy*, 7(10), 238–252. <https://doi.org/10.5897/jpp2015.0361>
- [43] Suma, A., Ashika, B. D., Roy, C. L., Naresh, S., Sunil, K. S., & Sathyamurthy, B. (2018). GCMS and FTIR analysis on the methanolic extract of red Vitis Vinifera seed. *World Journal of Pharmaceutical Sciences*, 106–113. <https://wjpsonline.com/index.php/wjps/article/download/gc-ms-ftir-analysis-red-vitis-vinifera-seed/352>
- [44] Kumar, B., Shah, M. A., Kumari, R., Kumar, A., Kumar, J., & Tahir, A. (2019). Depression, anxiety, and stress among final-year medical students. *Cureus*. <https://doi.org/10.7759/cureus.4257>
- [45] Yang, F., Chu, T., Zhang, Y., Liu, X., Sun, G., & Chen, Z. (2020). Quality assessment of licorice (*Glycyrrhiza glabra* L.) from different sources by multiple fingerprint profiles combined with quantitative analysis, antioxidant activity and chemometric methods. *Food Chemistry*, 324, 126854. <https://doi.org/10.1016/j.foodchem.2020.126854>
- [46] Yilmaz, F. (2020). Application of Glycyrrhiza glabra L. Root as a Natural Antibacterial Agent in Finishing of Textile. *Industrial Crops and Products*, 157, 112899. <https://doi.org/10.1016/j.indcrop.2020.112899>
- [47] Boçsan, I. C., Pop, R. M., Sabin, O., Sarkandy, E., Boarescu, P., Roşian, Ş. H., Leru, P., Chedea, V. S., Socaci, S., & Buzoianu, A. D. (2021). Comparative Protective Effect of Nigella sativa Oil and Vitis vinifera Seed Oil in an Experimental Model of Isoproterenol-Induced Acute Myocardial Ischemia in Rats. *Molecules*, 26(11), 3221. <https://doi.org/10.3390/molecules26113221>
- [48] Koçak, Ö. F., & Yilmaz, F. (2021). Use of Alpinia officinarum rhizome in textile dyeing and gaining simultaneous antibacterial properties. *Journal of Natural Fibers*, 19(5), 1925–1936. <https://doi.org/10.1080/15440478.2021.1889441>
- [49] Boender, J., Kruip, M. J., & Leebeek, F. W. (2016). A diagnostic approach to mild bleeding disorders. *Journal of Thrombosis and Haemostasis*, 14(8), 1507–1516. <https://doi.org/10.1111/jth.13368>
- [50] Arnout, J., Hoylaerts, M. F., & Lijnen, H. R. (2006). Haemostasis. *Handbook of experimental pharmacology*, (176 Pt 2), 1–41. https://doi.org/10.1007/3-540-36028-x_1
- [51] O'Donnell, J. S., O'Sullivan, J. M., & Preston, R. J. S. (2019). Advances in understanding the molecular mechanisms that maintain normal haemostasis. *British journal of haematology*, 186(1), 24–36. <https://doi.org/10.1111/bjh.15872>
- [52] Guerrero, C. G., & Ronsano, J. B. M. (2015). Physiopathology and treatment of critical bleeding: a literature review. *PubMed*, 39(6), 382–390. <https://doi.org/10.7399/fh.2015.39.6.8907>
- [53] Adiloğlu, S., Aktaş, A., Öz, A. Z., & El, H. (2018). Hemostatic effects of adrenaline and Ankaferd (blood stopper) during orthodontic attachment bonding. *Turkish Journal of Medical Sciences*, 48(6), 1234–1238. <https://dergipark.org.tr/tr/pub/tbtmedical/issue/41101/497095>
- [54] Badovinac, S., Glodić, G., Sabol, I., Džubur, F., Makek, M. J., Baričević, D., Koršić, M., Popović, F., Srdić, D., & Samaržija, M. (2023). Tranexamic Acid vs Adrenaline for Controlling Iatrogenic Bleeding During Flexible Bronchoscopy. *Chest*, 163(4), 985–993. <https://doi.org/10.1016/j.chest.2022.10.013>
- [55] Kelleş, M., Kalcıoğlu, M. T., Şamdancı, E., Selimoğlu, E., Iraz, M., Mıman, M. C., & Haznedaroğlu, İ. C. (2011). Ankaferd blood stopper is more effective than adrenaline plus lidocaine and gelatin foam in the treatment of epistaxis in rabbits. *Current Therapeutic Research*, 72(5), 185–194. <https://doi.org/10.1016/j.curtheres.2011.08.002>
- [56] Biranje, S., Sun, J., Shi, Y., Yu, S., Jiao, H., Zhang, M., Wang, Q., Jin, W., & Liu, J. (2021). Polysaccharide-based hemostats: recent developments, challenges, and future perspectives. *Cellulose*, 28(14), 8899–8937. <https://doi.org/10.1007/s10570-021-04132-x>